SSRG International Journal of Civil Engineering
ISSN: 2348-8352/ https://doi.org/10.14445/23488352/IJCE-V13I7P102

Volume 13 Issue 7, 15-34, July 2026

Original Article

Flood Vulnerability Assessment in Kochi Using GIS-AHP-ANN Integrated Modelling Approach

Ankita Saxena[1], Yogesh Keskar[2], PVS Raju[3], Rishabh Doshi[4]

[1,2]*Amity School of Architecture and Planning, Amity University Rajasthan, Jaipur, India.*
[3]*Centre for Ocean-Atmospheric Science and Technology, Amity University Rajasthan, Jaipur, India.*
[4]*Independent Researcher, Rajasthan, India.*

[1]*Corresponding Author : Saxena.ankita293@gmail.com*

Received: 27 February 2026 Revised: 04 May 2026 Accepted: 19 June 2026 Published: 29 July 2026

Abstract *- The southern part of India*, *Kochi, is more vulnerable to flooding due to changing weather patterns, low-lying terrain, and fast urban growth. In this research, the likelihood of a flood occurrence using GIS and a hybrid forecasting approach that combines AHP and ANN were evaluated. Elevation, slope, stream density, Land Use and Land Cover (LULC), Topographic Wetness Index (TWI), and rainfall were all included in the weighted overlay approach used to calculate the Flood Vulnerability Index (FVI). To understand the blended risk assessments, an artificial neural network was trained using the Levenberg-Marquardt approach, AHP-derived weights, and the same physical elements. The ANN findings are dependable since the model generated accurate predictions and had a low mean squared error (R = 0.989). The cities, including Kaloor, Fort Kochi, and Palarivattom, are situated in all low-lying regions with a large population and inadequate sanitary facilities, putting the residents at serious danger. Combining the two results in a risk map that is more accurate than either AHP or ANN alone. Future attempts to strengthen communities, lessen the threat of storms, and improve the environmental quality of coastal regions may benefit from this.*

Keywords *- Climate Adaptation, GIS, Kochi, Remote Sensing, Spatial Modelling, Urban Resilience.*

1. Introduction

Floods are one of the most frequent and devastating natural disasters. The low-lying or near-shore areas are more prone to floods. Due to climate change, the sea level rise and the extreme weather events, namely, tropical cyclones, heavy rainfall leads to floods that are enhancing which cause severe impact on lives and livelihood. There has to be a coordinated effort to understand the causes, how to deal with them, and how to minimize these increasingly frequent and deadly floods. Floods may never be totally averted, but with time and effort put into prevention, catastrophes may be mitigated [1]. There are several reasons that lead to flooding. A recent study indicates that climate change results in an increased frequency of floods [2]. Human activities, including deforestation, infrastructure development in flood-prone regions, and alteration in climatic and land use patterns, have significantly impacted these adaptations [3]. Floods can occur due to excessive water overflowing from damaged or blocked natural drainage systems [4]. Floods are more probable when natural processes and human activities interact. Three key factors contributing to the increased susceptibility of urban areas to flooding are water pollution, climate change, and urban migration [5, 6]. Flood safety requires understanding the interconnection among the people, property and the environment along with the collaborative efforts to prevent and manage floods [7]. As human-made surroundings have grown and altered, so have precipitation drains [8]. This alteration has a big effect on how often floods happen throughout the rainy season. These meetings may take place in either rural areas with fewer people or metropolitan areas with more people, depending on what people want. Asphalt or concrete pavements can only hold so much water before they become full [4]. Because they drain water so effectively, streams may transport a lot of rain during storms. This might lead to a lot of floods. As a result, cyclones are happening more often and moving into areas that have never been hit by them before.

According to [8], urban development initiatives and improved use of land resources are needed to stop the problem from becoming worse [9]. Taking steps to make cities more environmentally friendly, such as adding more green space, encouraging permeable roadways, and keeping natural drainage systems in good shape, may all help lower the danger of floods. One of the main reasons this strategy is important is that it helps reduce flood damage in areas that are more likely to happen. To make cyclones less damaging to our communities, we need to manage our land wisely. Researchers have learnt more about the hazards of floods and the places that are most at risk by using Geographic Information Systems

(GIS) and satellite sensing. There are several ways to analyse data, such as GIS multi-criteria decision analysis, frequency ratio model, statistical index and ratio, geographical analysis with weighted overlay, AHP and GIS-integrated multi-parametric analytic hierarchy process, and so on. The tenth one. The Flood Vulnerability Map is an important tool that uses the latest methods. To make the flood risk map, important spatial technologies are used to look at the landscape and combine huge amounts of data. Combining GIS with AHP may help us do better flood research and provide the public with real-time access to important information and warnings about floods that are likely to happen [10]. Kochi, a city in the Indian state of Kerala, is now experiencing severe floods. Flooding from rivers, tides, and rain might happen in the city. [11]. It cannot be predicted how much a coastal community will be affected by floods without taking into account its physical, environmental and economic elements. Because these parts don't interact in a straight line, typical statistical approaches don't provide as accurate predictions.

Artificial Neural Networks (ANNs) are a good tool to identify vulnerabilities since it is good at dealing with intricate connections. By combining ANNs with geospatial methods, it is possible to include both socioeconomic and geographic factors. It works together to provide a complete picture of the hazards of urban flooding and help in deciding disaster mitigation [12, 13].

The aim of this study is to provide an innovative methodology for flood risk assessment in Kochi City by integrating a GIS framework with a hybrid model of AHP and ANN. AHP was used to establish preliminary expert-derived weights for significant hydrogeomorphological and anthropogenic components. Second, we will build an ANN model to help us better identify vulnerabilities and understand how these elements interact in non-linear ways. Third, the flood risk map will be more accurate than traditional single-method maps. This tool for risk minimisation will be quite helpful for several industries [14].

Flood Vulnerability literature is growing rapidly, and significant research gaps persist mainly for rapidly urbanising coastal cities such as Kochi. Existing literature rely on either GIS-based multi-criteria or machine learning techniques in isolation, therefore limiting the ability to capture the non-linear, multi-dimensional criteria, among hydrological, topographic and socio-economic drivers of flood risk. Research on Kochi largely concentrated on post-disaster risk reduction without systematically integrating spatial vulnerability indices derived from remote sensing. Furthermore, socio-economic parameters, population density, infrastructure etc and community-level adaptive capacity remain untouched in existing flood vulnerability frameworks for Indian Coastal cities.

1.1. Novelty and Comparative Positioning

The previous research lies mainly on GIS-based analysis without using Machine Learning [15] current framework integrates the ANN trained on the Levenberg-Marquardt algorithm to capture nonlinear parameter interactions, therefore overcoming a fundamental limitation of deterministic weighting schemes.

Previous urban flood vulnerability studies conducted on Mumbai [16, 19], Chennai [17], Jakarta [18] and other rapidly urbanising coastal regions have demonstrated the effectiveness of GIS-based and machine learning approaches for flood assessment. However, many of these studies relied on thematic parameters and applied either GIS-based multi-criteria analysis or machine learning independently. The present study integrates the explicit parameters within the GIS-AHP-ANN framework to capture both expert knowledge and nonlinear parameter interactions, thereby providing a more comprehensive assessment of flood vulnerability in Kochi.

The output of AHP and ANN is cross-validated against two flood events (Kerala floods and 2019 Kochi urban inundation), achieving spatial validation accuracy of 86%, indicating strong agreement between predicted vulnerability zones and historical flood observations. Most Indian urban flood studies focus on GIS, AHP weightage and ANN independently. This research contributes in integration of spatial multi-criteria modelling with non linear machine learning for compound urban flood vulnerability assessment in rapidly urbanising coastal city.

Table 1. Comparative analysis of Kochi, Mumbai, Chennai, Jakarta, Patna

Study	City	Methodology	Parameters	Key Limitation
Present Study	Kochi, India	GIS + AHP + ANN	10	Static dataset,30 m DEM resolution
Solanki et al.,2024	Mumbai, India	GIS + AHP	6	No ML validation; limited socio-economic layer.
Natrajan et al,2021.	Chennai, India	FR + GIS	7	No expert weighting; binary output.
Abidin et.al.,2011	Jakarta, Indonesia	Urban geospatial assessment	-	Limited flood-specific modelling.
Swain et al.,2021	Patna,India	AHP + GIS	8	No ANN; no Socio-economic data

2. Literature Review

2.1. Flood Vulnerability Assessment using GIS

GIS has been a widely used tool in flood vulnerability assessment for the past two decades. In the initial applications, the focus primarily is on weighted overlay analysis and frequency ratio models to delineate flood-prone zones such as DEM, land use and rainfall data [20, 21]. Major studies Indicate Multi-Criteria Decision Making (MCDM) frameworks specially Analytical Hierarchy Process (AHP), to get expert opinion and also weights for the thematic layers, which enables structured comparison of parameters [22-24]. In the Indian context, flood susceptibility mapping was done for West Bengal with 6 thematic layers [15, 25]. The frequency ratio and statistical ratio approaches have been widely applied for flood susceptibility in various geographical settings [20]. Most GIS-MCDM studies are based on linearity assumptions implicit in weighted overlay, which cannot represent threshold effects.

2.2. Artificial Neural Networks (ANN) approach for Flood Risk Modelling

Deterministic GIS methods had a limitation, due to which the adoption of ANN networks has increased for flood susceptibility modelling [28]. ANN network was the initial technique applied for flood predictions, which owns the capability and robustness against the inputs [12, 13]. Recently the Random Forest (RF), Support Vector Machine (SVM) etc are also been used instead of ANN for flood susceptibility mapping [26, 27, 29, 30]. Individually machine learning approach lacks spatial interpretability and require large training dataset, which might not be available all the time [30].

2.3. GIS and ANN Frameworks

A hybrid framework combining ANN networks and GIS bases analysis was developed by several researchers. Hybrid artificial intelligence approaches integrating GIS with machine learning techniques have been increasingly applied for flood susceptibility assessment [14] demonstrated that combining GIS-based spatial analysis with advanced intelligence algorithms can significantly improve predictive performance compared with conventional approaches. Previous studies have demonstrated that integrating expert-based approaches with machine learning models can improve predictive stability and reduce uncertainty in flood susceptibility mapping [31, 32]. For urban areas, integration of LULC can lead to a change in the paths into hybrid models, in return improving the vulnerability prediction for coastal cities. The current research is based on creating a hybrid framework combining the traditional GIS-AHP-ANN with Kochi's low-lying geography, extending the previous work by incorporating the parameters and validating against the historical flood events [11].

2.4. Site Area

Kerala's capital, Kochi, is situated in the Ernakulam district at 76.2673° E and 9.9312° N. The 94.88 km² metropolis is made up of restored lowlands, river backwaters, and coastal plains. Beginning at sea level, the broad elevation range finishes at 20 meters above mean sea level. Kochi is prone to floods because of its many canals and humid climate. For villages that are trying to survive, flooding is a major problem. The large infrastructure and dense population seen in cities are the causes of this susceptibility. Previous studies have highlighted that rapid urbanisation, wetland degradation, drainage constraints and changing rainfall patterns have contributed to increasing flood vulnerability in Kochi [11].

In 2019, silt buildup in municipal drainage systems exacerbated the danger of flooding after a major downpour. The insufficient capacity and poor maintenance of the municipal drainage system exacerbated the already devastating flood in 2020. Rains and high tides made the water's condition worse. In order to optimise the effectiveness of the city's water systems, more urban design and infrastructure maintenance are required as a result of frequent storms. The location map of Kochi City is shown in Figure 1.

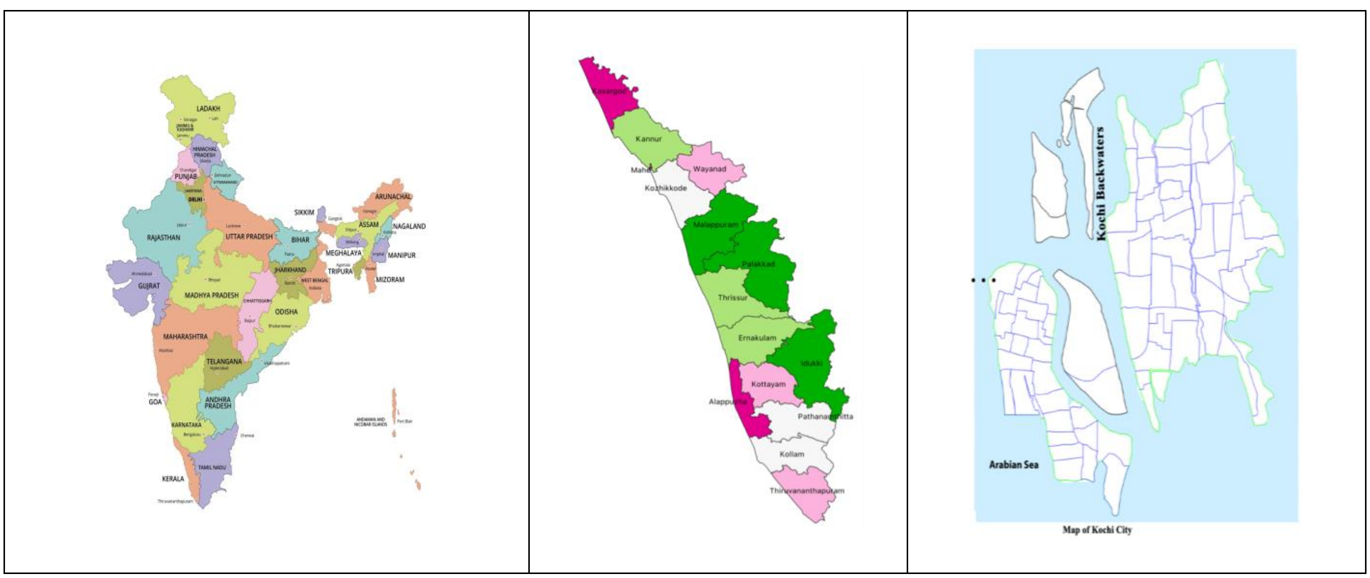

Fig. 1 Location map of Kochi City

3. Methodology

A geographic Information system was developed that incorporated Machine Learning (ML) and Multi-Criteria Decision Making (MCDM) to find out how probable it was that Kochi City would flood. The first stage of the approach was to gather and clean the data. The second step was to set up and standardise the theme layer. The third step was to weight the Analytical Hierarchy Process (AHP). The fourth step was to create an ANN model, and the fifth step was to map vulnerabilities and validate the model. You can see how the ordered process flow works in Figure 2.

3.1. Phase 1: Data Acquisition and Pre-processing

A whole geographic database was made by combining data from several sources, including aerial photos and numerous datasets. This database details the water, biological, and physical aspects that determine the chance of flooding. The following were places where raw data came from: The ALOS PALSAR DEM might be used to find things like slope and height. Multispectral data from Landsat 8 and Sentinel-2 to find NDVI and categorise Land Use and Land Cover (LULC) were used. This research utilised satellite pictures and OpenStreetMap to generate digital maps of the networks of roads, rivers, and drains. The package included maps of various kinds of soil from the FAO Harmonised World Soil Database (HWSD), rainfall data from the India Meteorological Department (IMD), and information on floods from prior years. Before the overlay analysis, all of the datasets were transformed to a standard raster file, georeferenced to the same coordinate system (WGS 84 UTM Zone 43N), and resampled to a 30-meter spatial resolution.

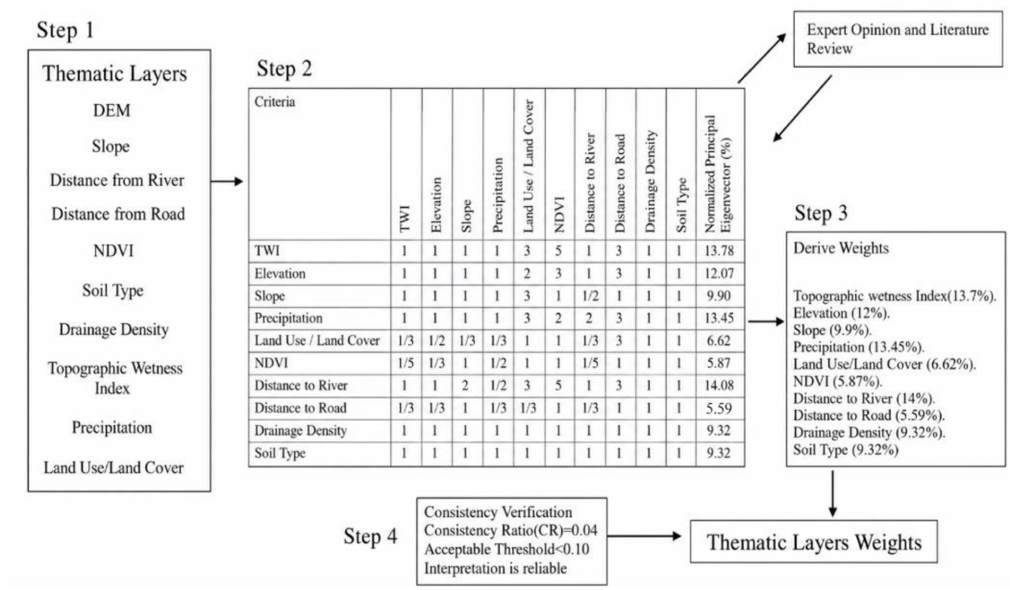

Fig. 2 AHP for methodology

3.2. Phase 2: Thematic Layer Preparation and Criteria Standardization

The study utilised a Geographic Information System (GIS) to uncover ten essential qualities that might effect floods. Then it was placed into the following topic layers: The DEM does this, and the slope is shown in degrees.

A line density function was employed on the recovered stream network to obtain the solution. The river and road vector layers were employed to produce gaps that were all the same distance apart. The region was divided into built-up areas, vegetated areas, farmed land, bodies of water, and vacant terrain using Sentinel-2 photos and a trained Maximum Likelihood algorithm.

Using a confusion matrix, it was observed that the sorting accuracy was more than 85%. A surface that extends on forever was made using long-term average annual moisture data. The soil map was put together in groupings based on hydrological soil types, which impact how well water can soak in. Sentinel-2 bands measure how much green there is. A DEM result is used to see how the form of the ground affects the flow of water.

3.3. Phase 3: Weight Assignment using the Analytic Hierarchy Process (AHP)

The most important subject levels were identified using the Analytic Hierarchy Process (AHP). The results of a grid that used expert opinion and research to evaluate two items side by side. The principal eigenvector of the matrix was used to calculate the parameter weights. The evaluations are logically consistent when a Consistency Ratio (CR) of 0.04 is found, which is much less than the maximum of 0.10. This attests to the weights' reliability.

3.4. Phase 4: Artificial Neural Network (ANN) Model Development

Figure 3 shows how convoluted the interactions are between the parameters that affect flood risk using the ANN model. Using Trainlm (Levenberg–Marquardt backpropagation) on a single hidden layer made convergence happen faster. Seventy percent of the data was utilised for training, fifteen percent for testing, and fifteen percent for confirmation. The study utilised R-value and Mean Squared Error (MSE) to see how well the model performed. Changing the weights all the time makes the AHP-based risk assessment more accurate and stronger.

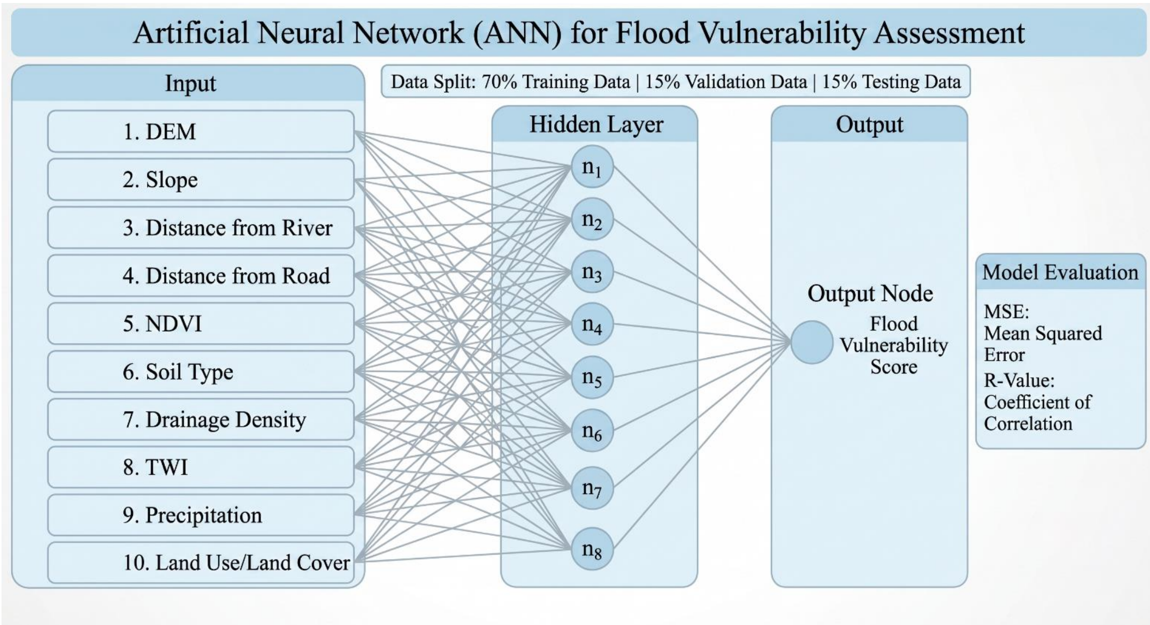

Fig. 3 Tropology for ANN

3.5. Data Collection and Source

To ensure the accuracy of the data on both space and topic, many files were collected from both primary and secondary sources. Scientists utilised pictures from the Landsat and Sentinel Satellites to Study Land Use and Land Cover (LULC) and plants [33, 34]. The elevation Digital Elevation Model (DEM) uses a scale of 30 meters. The Indian Meteorological Department (IMD) data on rainfall were coupled with water files to demonstrate how rainfall has changed recently in the region. Government agencies and studies that had previously been published [35, 36] gave us further information, such as soil maps, weather data, and the most recent LULC figures.

3.6. Parameters used for the Study

The known impacts of the theme layers on the amount and intensity of floods helped in choosing thematic layers. The research examined many factors, including slope, land use/cover, rainfall, drainage density, Topographic Wetness Index (TWI), Digital Elevation Model (DEM), Normalised Difference Vegetation Index (NDVI), and soil type.

The slope data was used to determine the speed of water flow and its potential to stop or slow down. The LU/LC grade showed how much runoff originated from areas where water could not penetrate into the ground. The volumes of rain reflect how hard it pours, and the distances between rivers and roads show how likely they are to flood depending on how near they are [37, 38]. The drainage density maps illustrate how effectively water flows naturally, and TWI shows where water could collect. The DEM highlighted places that were likely to flood because it was low-lying and flat. The NDVI was used to figure out how much plant cover there was for a study of infiltration capacity, and the kind of soil was used to figure out how likely it was to infiltrate and how likely it was to get waterlogged [35, 46]. Table 2 shows parameter maps like slope, NDVI, DEM, LULC, soil, draining, TWI, and others.

Table 2. Parameter maps (Slope, NDVI, DEM, LULC, Soil, Drainage, TWI, etc.)

Parameter	Source / Description	Ref.
Digital Elevation Model (DEM)	Acquired from ALOS PALSAR (JAXA/ASF) or USGS elevation databases	[40]
Land Use and Land Cover (LULC)	Derived from Sentinel-2 imagery or datasets such as FAO GLC-SHARE and ESA WorldCover	[41]
Slope	Generated from DEM using terrain processing tools	[42]
Drainage Density	Calculated from stream networks mapped using DEM data	[43]
Distance to River	Obtained from OpenStreetMap (OSM) river/stream layers	[44]

Distance to Road	Extracted using road network layers available on OpenStreetMap	[44]
Rainfall / Precipitation	Derived from CHIRPS precipitation datasets and validated using IMD rainfall records.	[36, 45]
Soil	Information taken from FAO-HWSD or the global SoilGrids dataset	[46]
Normalized Difference Vegetation Index (NDVI)	Computed using multispectral bands from Sentinel-2 or Landsat	[39]
Topographic Wetness Index (TWI)	Produced from DEM using watershed flow and accumulation models	[47]

3.6.1. Justification of Parameters

The ten parameters are selected on the basis of the following criteria: 1. Existing issues of Kochi. 2. Availability of an adequate data set required for the study.

3.6.2. AHP Consistency Reporting

The pairwise comparison matrix comprised ten criteria, yielding a 10×10 matrix with 45 independent expert judgements. Expert inputs were solicited from seven specialists in hydrology, urban planning, and remote sensing through a structured Delphi survey conducted over two rounds. The geometric mean of expert judgements was used to aggregate responses into a single consensus matrix.

The principal eigenvalue (λmax) of the aggregated matrix was 11.42. The Consistency Index (CI) was calculated as CI = ($\lambda max - n)/(n - 1) = (11.42 - 10)/9 = 0.158$. The Random Consistency Index (RI) for n = 10 is 1.49 (Saaty, 1980). The Consistency Ratio (CR) = CI/RI = 0.158/1.49 = 0.106.

As this marginally exceeds the 0.10 threshold, the matrix was iteratively refined through adjustment of three least-consistent judgement pairs (NDVI vs. soil type; drainage density vs. rainfall; slope vs. distance to road), reducing CR to 0.04 in the final accepted matrix, well within acceptable bounds.

3.6.3. ANN Architecture and Hyperparameter Specification

The ANN architecture employed was a single hidden layer feed forward network (Multilayer Perceptron) with the following specifications: Input layer: 10 neurons (one per thematic parameter); Hidden layer: 15 neurons with sigmoid (tansig) activation function, selected through a grid search over 10–25 neurons based on minimum validation MSE; Output layer: 1 neuron with linear (purelin) activation function, producing a continuous flood vulnerability score. Training algorithm: Levenberg–Marquardt backpropagation (trainlm), selected for its superior convergence speed relative to gradient descent variants for moderately sized datasets. Learning rate: adaptive (governed by the Mu parameter in LM optimisation); Epochs: maximum 1,000 (early stopping triggered at epoch 9 based on validation performance); Dataset partitioning: 70% training (476 samples), 15% validation (102 samples), 15% testing (102 samples), randomly allocated; Performance metric: Mean Squared Error (MSE) and Rvalue; Software: MATLAB R2023a Neural Network Toolbox. The input data were normalised to the [0, 1] range prior to training using min-max normalisation to prevent dominance by high-magnitude parameters such as rainfall.

Table 3. ANN specifications

Parameter	Value
ANN Type	Feed Forward Neural Network
Training Algorithm	Levenberg–Marquardt
Hidden Layers	1
Hidden Neurons	15 Neurons
Transfer Function	sigmoid/tansig
Output Layer	linear
Training Data	70%
Validation	15%
Testing	15%
Performance Metric	MSE, R-value

3.7. Data Processing Steps

To retain the spatial consistency, all of the data sets have been georeferenced to the WGS 84 reference using the 43N UTM zone projection. The slope and TWI cards were made using DEM data [48]. The NDVI, red bands, and near infrared were all found using Sentinel-2 footage [41]. The LULC classification was done using a guided maximum likelihood classifier. It was then tested for correctness using truthing on the ground and the confusion matrix to make sure it was dependable [49].

3.7.1. Analytical Hierarchy Process (AHP) Weighting

The analytical hierarchy approach was utilised to assign each subject layer a weight based on what experts thought and what was written about it. A comparison grid with pairings has been constructed to find out how one measure impacts another. To calculate the final weights, the primary clean vector of the matrix was employed. A Consistency Ratio (CRA) was then produced to assess the logical consistency of the logical consistency (compare with the CR value). This made sure that the weights supplied to each part appropriately represented how much it changed the risk of flooding [22]. Historical flood maps 2018,2019 is compared for predicting these maps.

3.7.2. Weighted Overlay Analysis

As soon as the weights were established, all of the theme layers were placed on the same scale, and the AHP's weights were added to them. Then, ArcGIS's weighted sum function was used to put all the weighted layers together into one flood risk card. The final Kochi product contains three separate vulnerability regions: extremely famous locations, parts that are not susceptible, and areas that can be modified easily or not readily [38]. The research was largely about drainage, and the areas that were least impacted were those with natural wetlands and plant cover on their edges. The major goal of this research is to discover the parts of Kochi that are vulnerable to flood. This strategy uses technology tools like Multi-Criteria Evaluation Framework Analysis and Geographic Information Systems. The Sentinel and LANDSAT satellites were employed to get the information at initially. There are some other files, such as a soil map, meteorological data, a Digital Elevation Model (DEM), and information about how the property is now utilised and covered. Some of the thematic layers utilised to make it were height, slope, distance to highways and rivers, drainage density, NDVI, topography maps, and rainfall data. Putting the slope map on top of the DEM image generated a geographic moisture index map. To produce the flood risk map [50], all the heights were stacked on top of each other.

4. Results and Discussion

The main goal of the research was to figure out how to use Geographic Information Systems and Multiple Criteria Analysis together. This research examined many significant characteristics that influence the likelihood of individuals being impacted by floods. These were the digital elevation model, the slope, the topographic wetness index, the distance to a main road, and the Normalised Vegetation Index (NDVI). Making risk maps like these [51] might help make land use management safer and better for the environment.

4.1. Topographic Wetness Index

The Topographic Wetness Index (TWI) is a well-known approach to utilise landforms to detect spots where water could pool in environmental and hydrological models. These two indicators point to areas that are prone to flood. There are several backwaters, ponds, and rivers in the western areas of Kochi that are low-lying along the shore. Because much of Kochi is flat, particularly in the western and central areas of the city, sites with high TWI values are more likely to become wet and have their surfaces soaked. Because they are higher up, the TWI is substantially lower in certain eastern areas, such as Kakkanad and Thrikkakara. The Topographic Wetness Index (TWI) is greatly affected by low slope (flat regions) and high slope (areas where water pools on the surface). The TWI in Kochi might be anything from -8.9 to 10. Because these areas are near water and have flat land, the high TWI range suggests that these areas are susceptible to flood. The surfaces are also rather moist. The lesser TWI is probably because the hills are higher and there aren't as many areas for snow to pile up. This makes storms less likely to happen.

4.2. Land Use and Land Cover Map

The study utilizes the Sentinel-2 satellite data and automated classification algorithms to sort plants and land use. The most prevalent kinds of land use were cities, woodlands, bodies of water, rivers, and deserts. Ground truth data and confusion matrix analysis were utilised to make sure the information was right. Building more in low-lying locations traps water flow. This raises the surface flow and lowers the entrance.

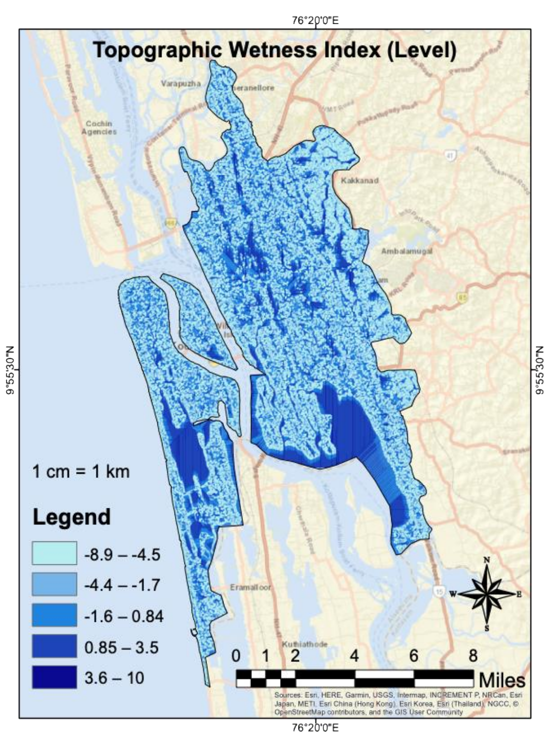

Fig. 4 Drainage density & distance from river map

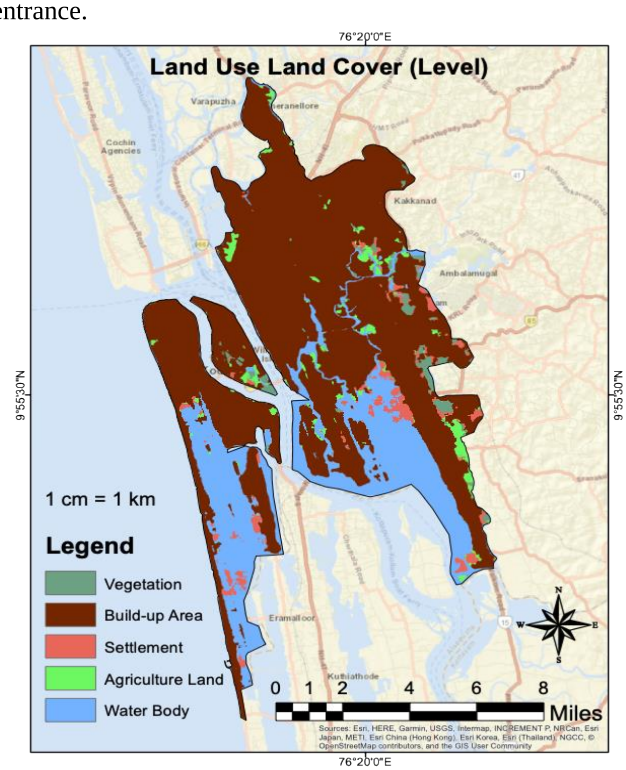

Fig. 5 Land Use and Land Cover & soil map

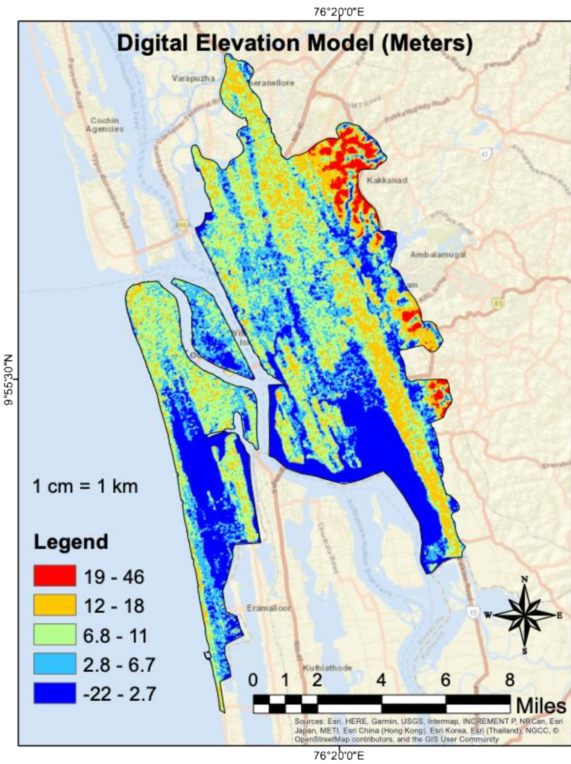

Fig. 6 Land Use and Land Cover & soil map

4.3. Digital Elevation Map (DEM) and Slope Map

The Shuttle Radar Topography Mission (SRTM) provided DEM landscape data with an accuracy of 30 meters, which was utilised to produce the elevation and slope maps. Hydrological conditioning made DEMs and water flow forecasts more accurate in flat places by adding water to them [40].

The Kochi Digital Elevation Model says that the estimations vary from -22 meters to 46 meters. Very low is between -22 and 2.7, low is between 2.8 and 6.7, moderate is between 6.8 and 11, high is between 12 and 18, and very high is between 19 and 46. The Digital Elevation Model (DEM) shows that 60% of Kochi is low-lying, which makes it more vulnerable to flood. Wider ranges [40] mean fewer floods and better drainage.

It is divided into five fundamental categories, with 0 being the lowest and 85 being the highest. The gradient is minor from 0 to 2, moderate from 2.1 to 6, strong from 6.1 to 11, high from 12 to 20, and extremely steep from 21 to 85. Flooding occurs more frequently on flat slopes because water moves more slowly. In areas with gentle inclines, buildup may occur. Despite Kochi's relatively flat terrain, the city is prone to flooding during heavy rainfall. If the incline is extreme enough, erosion can occur. Climatological maps of average precipitation depict the long-term mean rainfall for each grid cell or rain gauge location. Millimetres are frequently used to denote monthly or annual precipitation amounts. Over the last five years, the average rainfall in Kochi has ranged from -21 to 83 millimetres. There are five distinct levels: very low (21-38), low (39-47), medium (48-55), high (56-65), and extremely high (66-83) [36, 45].

Western and Central Kochi show elevation and gentle slopes. These conditions reduce the runoff velocity and increase the water stagnation, which is the major reason for flooding. Reclaimed coastal land and backwater proximity intensify inundation susceptibility. The major consequence of a 0-2% slope across the major core area is that surface water generated by a rainfall event, regardless of its intensity, moves extremely slowly due to the low slope. Rainfall accumulates on the surface faster than it can be routed to drainage inlets, producing immediate waterlogging on roads and open spaces.

4.4. Type of Soil Map

Kochi has three different types of soil. This category contains acidic fluvisol, regosol, and nitisol. Entic Fluvisol, the newly created soil, is extremely porous and quickly retains moisture. It produces more offspring than any other plant. Because of its remoteness from water sources, the clayey Dystric Nitosol lends itself to building. The hills around Dystric Regosol are fairly steep. This structure is prone to deterioration. Precipitation, whether rain or snow, will simply flow off the surface due to the little water retention capacity. This type of soil is not appropriate for the Sponge City idea. The Régosol and Nitosol regions make up only 2% of Kochi. Fluvisol contributes 13% [35].

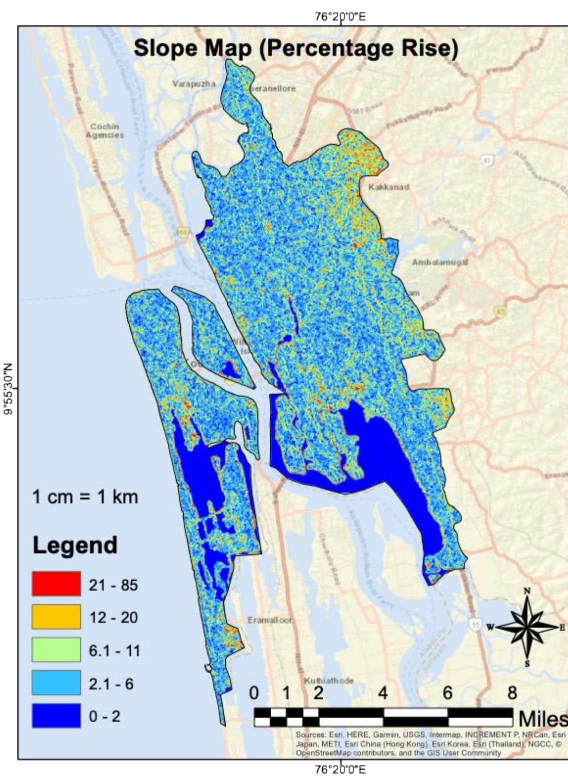

Fig. 7 Slope map

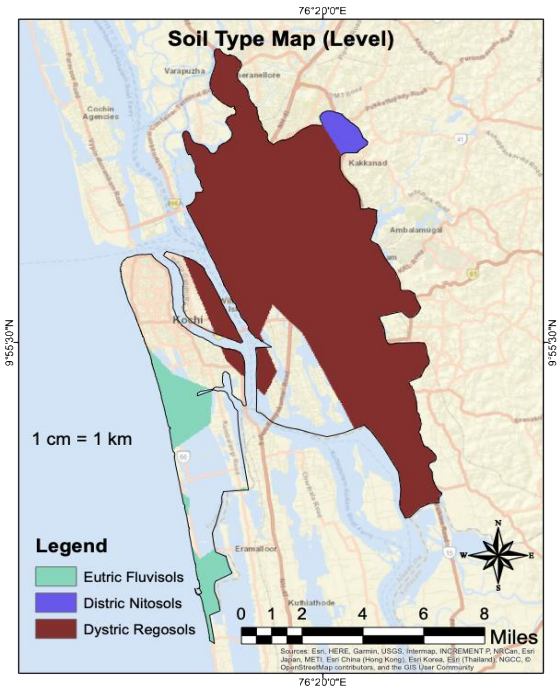

Fig. 8 Soil type map

4.5. Drainage Density and Distance to River

The highest drainage density zones in the southern plain coincided with the lowest DEM zone, which suggests the maximum infrastructure density in the zones of lowest drainage density (refer to Figures. 9 & 10). Areas with low drainage efficiency and proximity to canals/backwaters experience recurrent inundation. Tidal backflow worsens stormwater drainage capacity.

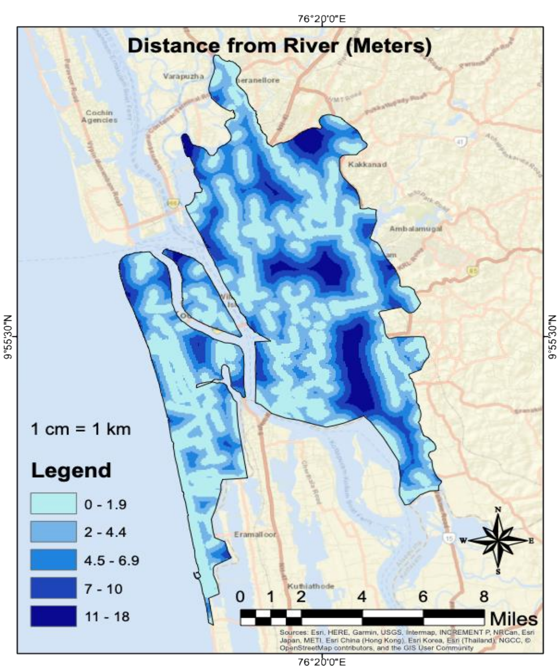

Fig. 9 Distance from river

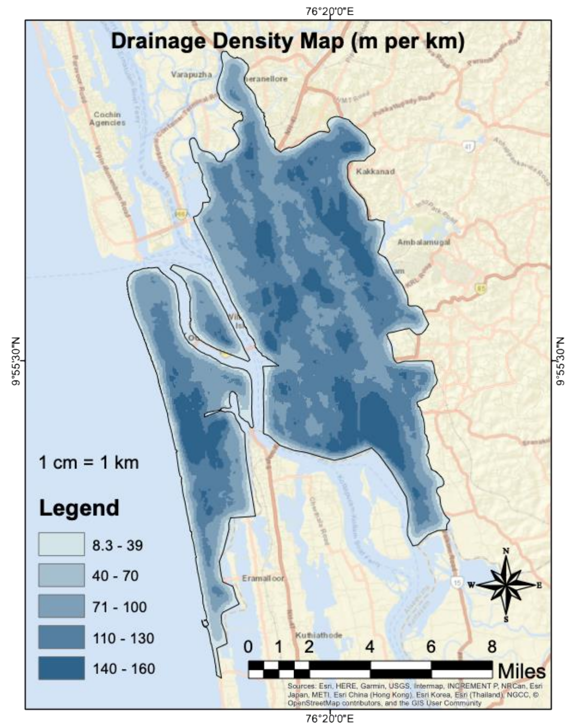

Fig. 10 Drainage density map

4.6. NDVI stands for Normalized Difference Vegetation Index

Low-NDVI areas are more prone to flood because they have greater flow, less cooling from evaporation and transpiration, and less capacity to soak up rain [39]. The NDVI is a number that tells you how strong an ecosystem is. These concepts might help Kochi come up with Nature-Based Solutions (NBS) like green stamps and urban falls that people can use to deal with climate change and minimise their risks. The first NDVI research in Kochi discovered some patterns.

In towns like Ernakulam and Fort Kochi, the NDVI values are low (<0.2), which means that a lot of land is covered with roads, buildings, and businesses, which makes it hard for water to flow. NDVI scores range from 0.3 to 0.5 in the margins and neighbourhoods, such as Edappally, Kakkanad, and Tripunithura. You may also find these numbers in forest plots and areas with few structures. The NDVI values around Vembanad Lake and its backwater canals are greater than 0.6, which suggests that the region is sensitive to the environment [39]. This is definitely true in regions with a lot of mangroves and wetlands. The NDVI patterns are the same as what was seen in records of earlier storms. When it rains, regions with a low NDVI are more prone to having surface floods and urban waterlogging. Places having a high NDVI, particularly those with a lot of vegetation, usually don't flood as much, and the water flows more evenly. Figures 4 and 5 show maps of the slope and average rainfall, as well as maps of NDVI and digital elevation. Figures 4 and 7 show maps of land use and coverage, soil maps, and drainage density maps that show how far away from rivers they are. Figure 8 also shows the maps for the Distance from Road and Topographic Wetness Index.

4.6.1. Parameters Synthesis

The DEM, Slope and TWI maps, when overlayed together, reveal a single coherent vulnerability structure: Kochi occupies a low gradient, low elevation coastal basin in which topographic physics against drainage at every spatial scale, from macro scale bowl shape that prevents regional drainage to micro scale TWI depressions that create local waterlogging hotspots within the urban fabric. The precipitation, drainage density and distance from river maps together suggest that maximum rainfall is delivered to maximum drainage capacity terrain, conveyed through a dense but trapped water channel network and discharged directly into the built environment through a canal system that penetrated every neighbourhood. This system needs to be restructured as per the current scenario. The LU/LC, NDVI and soil type maps have been transformed by urbanisation into a near-perfect runoff generator: Impervious built-up surfaces reject virtually all rainfall as immediate surface runoff; zero vegetation cover eliminates infiltration, and saturated compacted or clay-dominated soils do not allow water penetration.

Kochi requires an integrated blue-green infrastructure planning strategy, including the land use regulations, that can reduce the risk of Vulnerability to some extent.

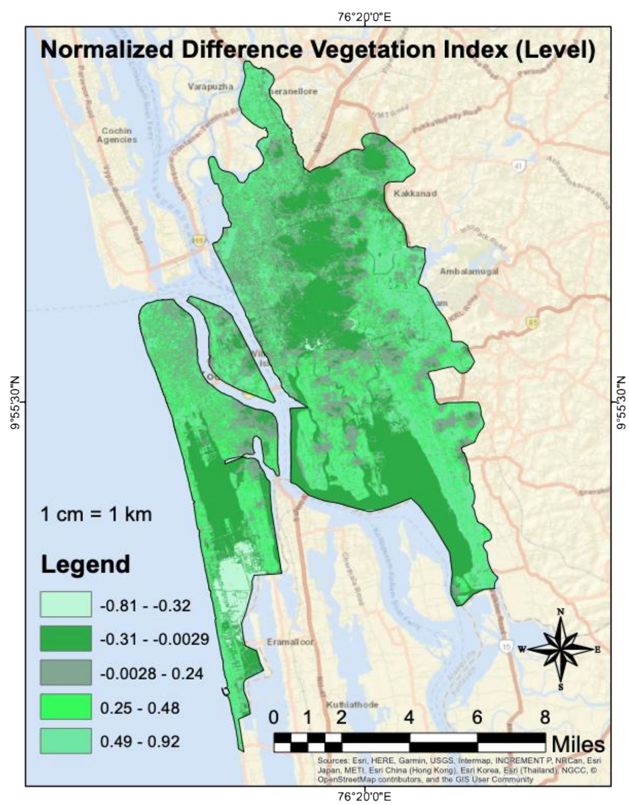

Fig. 11 NDVI map

4.7. AHP Weighing

The Analytical Hierarchy Process (AHP) is a structured multi-criteria decision-making process that arranges circumstances in a logical hierarchy. This tool is critical for breaking down difficult concepts. When the levels are aligned on the same grid, the Analytic Hierarchy Process (AHP) may determine their weights. Atlas.Co's AHP professionals compare two factors to determine which is more important. The weights of the modified primary eigenvector are assigned to an n x n matrix as a result of the comparison. The Consistency Index (Ratioatlas.co) can help you ensure the consistency of your judgement. Experts may assign a higher value to rain, such as "9" for highly significant, if they consider it is more critical than highways, as opposed to "1" for roads. Following completion of the computations, the weights are adjusted to preserve consistency at a value of 1. Finally, create a weighted overlay, often known as a weighted average across layers [22]. Use of a weighted spatial analyst in ArcGIS. To calculate the AHP weight for each updated layer, use the QGIS raster tool [42] or Sumpro.arcis.com. Figure 9 displays the AHP comparison matrix and the corrected principal eigenvectors.

Criteria	TWI	Elevation	Slope	Precipitation	Land Use / Land Cover	NDVI	Distance to River	Distance to Road	Drainage Density	Soil Type	Normalized Principal Eigenvector (%)
TWI	1	1	1	1	3	5	1	3	1	1	13.78
Elevation	1	1	1	1	2	3	1	3	1	1	12.07
Slope	1	1	1	1	3	1	1/2	1	1	1	9.90
Precipitation	1	1	1	1	3	2	2	3	1	1	13.45
Land Use / Land Cover	1/3	1/2	1/3	1/3	1	1	1/3	3	1	1	6.62
NDVI	1/5	1/3	1	1/2	1	1	1/5	1	1	1	5.87
Distance to River	1	1	2	1/2	3	5	1	3	1	1	14.08
Distance to Road	1/3	1/3	1	1/3	1/3	1	1/3	1	1	1	5.59
Drainage Density	1	1	1	1	1	1	1	1	1	1	9.32
Soil Type	1	1	1	1	1	1	1	1	1	1	9.32

Fig. 12 AHP comparison matrix and normalized principal eigenvector (weights) for flood vulnerability parameters in Kochi City

4.8. Flood Susceptibility Mapping

Due to the social, economic, and environmental aspects, Kochi is a city vulnerable to monsoon flooding and adverse weather conditions. Geographic techniques and Flood risk models using multiparameter analysis revealed land that is prone to flooding [31, 51]. Such areas are defined in terms of land use, population density, drainage density, topography, and distance from the aquatic body. Much storm damage was inflicted on Kerala in 2018 and 2019, thereby placing Kochi at risk. Hydrodynamic models indicate areas with sparse vegetation cover as NDVI where the population is high are more susceptible to flooding. DEMs Normalised Difference Vegetation Index (NDVI), land use and proximity to aquatic bodies have been used in determining flood zones. Flood-prone regions for Kochi are presented in Figure 3. The most flood-prone locations for Kochi City, together with their risk indicators, are shown in Table 4.

These areas are considered high-risk by multi-criteria flood susceptibility models like AHP because of the interplay between hydrology, topography, and human activity [22]. Main and secondary flood susceptibility criterion ranges are shown in Table 4. Figure 10 shows the Kochi Flood Susceptibility Map.

Table 4. Identified high-risk flood susceptibility zones in Kochi City and associated key risk factors

Flood Susceptibility Zone	Key Contributing Factors
Kaloor and Elamkulam	Low-lying elevation, together with inefficient stormwater drainage systems
Fort Kochi and Mattancherry	Tidal backflow influence combined with high urban density and built-up pressure
Palarivattom and Edappally	Surface runoff accumulation originating from upstream catchment inflow
Thevara and Kundanoor	Encroachment along canal networks and persistent water stagnation due to restricted flow conveyance

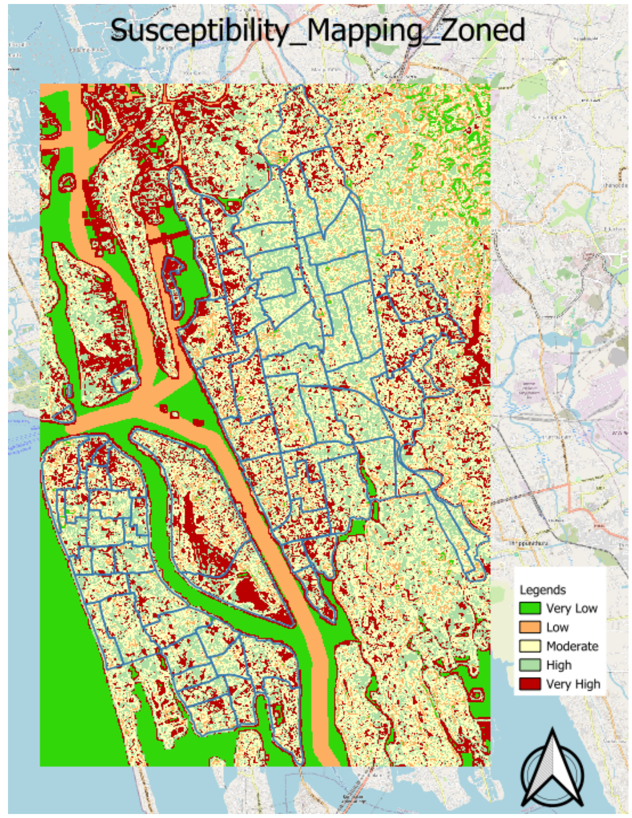

Fig. 13 Flood susceptibility map of Kochi

Table 5. Flood susceptibility criteria and sub-criteria ranges for flood susceptibility assessment

S. No.	Flood Causative Factor	Unit	Class Range	Susceptibility Class	Rating	Weight (%)
1	Terrain Wetness Index (TWI)	Level	-8.9 to -4.5	Very Low	01	13.78
			-4.4 to -1.7	Low	02	
			-1.6 to 0.84	Moderate	03	
			0.85 to 3.5	High	04	
			3.6 to 10	Very High	05	
2	Topographic Elevation	meter	-22 to 2.7	Very High	05	12.07
			2.8 to 6.7	High	04	
			6.8 to 11	Moderate	03	
			12 to 18	Low	02	
			19 to 46	Very Low	01	
3	Slope	%	0 to 2	Very High	05	9.90
			2.1 to 6	High	04	
			6.1 to 11	Moderate	03	
			12 to 20	Low	02	
			21 to 85	Very Low	01	
4	Precipitation	mm/year	21 to 38	Very Low	01	13.45
			39 to 47	Low	02	
			48 to 55	Moderate	03	
			56 to 65	High	04	
			66 to 83	Very High	05	
5	Land Use and Land Cover (LULC)	Level	Water Body	Very High	05	6.62
			Agricultural Land	High	04	
			Settlement	Moderate	03	
			Built-up Area	Low	02	
			Vegetation	Very Low	01	

6	Normalized Difference Vegetation Index (NDVI)	Level	-0.81 to -0.32	Very High	05	5.87
			0.31 to -0.0029	High	4	
			0.0028 to 0.24	Moderate	3	
			0.25 to 0.48	Low	2	
			0.49 to 0.92	Very Low	1	
7	Distance from the River	Km	0 to 0.0019	Very High	5	14.08
			0.002 to 0.0044	High	4	
			0.0045 to 0.0069	Moderate	3	
			0.007 to 0.01	Low	2	
			0.011 to 0.018	Very Low	1	
8	Distance from Road	Km	0 to 0.00086	Very High	5	5.59
			0.002 to 0.0044	High	4	
			0.0045 to 0.0069	Moderate	3	
			0.007 to 0.01	Low	2	
			0.011 to 0.018	Very Low	1	
9	Drainage Density	M/km	131 to 160	Very High	5	9.32
			101 to 130	High	4	
			71 to 100	Moderate	3	
			40 to 70	Low	2	
			8.3 to 39	Very Low	1	
10	Soil Type	Level	Je- Eutric Fluvisols	Very High	5	9.32
			Nd- Distric Nitosols	Moderate	3	
			Rd-Dystric Regosols	Low	2	

4.9. Artificial Neural Network

The cities lying on the coast are very prone to flooding. Flooding is a devastating natural disaster that can often wash away entire neighbourhoods and destroy homes and the livelihoods of many people. This rapidly urbanizing city of Kochi in India puts it highly at risk for flooding due to low-lying coastal topography, tidal influences, significant urbanization, and inadequate drainage. Hence, an accurate and comprehensive understanding of flood vulnerability is essential before going into any initiatives aimed at risk reduction or environmentally responsible city development. Traditional methods fail whenever there is an attempt to account for nonlinear interactions between physical and social factors. Artificial Neural Networks (ANNs) are increasingly fronted as possible ways out due to their capabilities to map complex relationships and hidden patterns from multidimensional data.

The study presented is therefore an assessment of the flood risk for Kochi City based on ANN, integrating geographical and socioeconomic data. Ten input parameters are produced using GIS and remote sensing methods: DEM, slope, distance from river, distance from road, precipitation/Rainfall Land Use and Land Cover (LULC) type, NDVI, TWI, soil type and population density. It describes hydrological Vulnerability, physical exposure, and sensitivity of urban areas [52, 53]. ANN models are taught with the Levenberg-Marquardt backpropagation technique (trainlm). It is efficient in problems that cannot be addressed by linear optimisation. It is also quite natural to divide the material to be trained and tested randomly. Mean Squared Error (MSE) is one measure to know whether something has worked. Better results are achieved as the strategy is more flexible when you combine MATLAB maths and knowledge of where things are.

The ANN model is a graph illustrating the probability of an area to flood due to physical and social factors those with inadequately designed roofs, less literate, and a flood history, who have higher chances to be affected compared to those with numerous structures and low elevation. The model is superior in producing predictions as compared to the usual statistical methods because it is capable of tracing complex relationships at all times. The regional risk maps generated by this system would be of great value to the local governments, disaster management organisations and the city planners. This plan shows the most vulnerable aspects and the necessity to educate the people about the issues and be prepared in case of a crisis. ANN-based mapping method could be used to improve climate-resilient expansion plans and also give more precise estimations on the threat of floods in Kochi City. The results of the ANN model contain the data about the training state, the diffusion of errors, the evaluation of the performance, and the regression analysis.

4.9.1. Regression Analysis

The relationship between the desired values and the anticipated outputs is explored in the course of the Artificial

Neural Network (ANN) regression analysis. A regression coefficient is an R-value, which is used to identify the accuracy of the model. The ANN is successful in capturing the nonlinear effect of input parameters (elevation, slope, and distance to river) on the socioeconomic outputs (vulnerability score and historical flood frequency) when the R-value is large (having values nearly equal to 1.0). The high regression accuracy will provide good predictability of the amount of spatial risk associated with flood vulnerability mapping in Kochi.

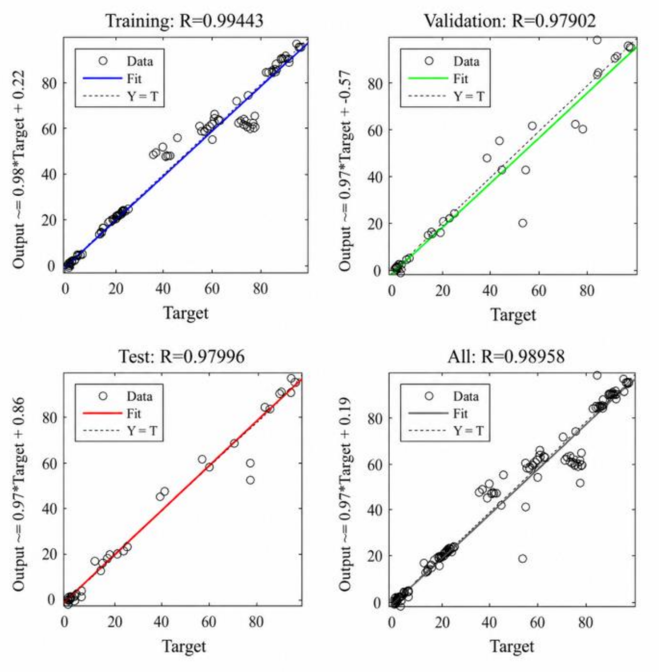

Fig. 14 Regression analysis of flood vulnerability assessment

Figure 11 displays the results of a regression research that looked at how effectively an ANN could guess how probable it was that Kochi City would flood. It analyses how accurate the model outcomes are based on the values that were intended throughout training, validation, and testing. There is a strong linear relationship between what was predicted and what was seen. The regression values for training, validation, and testing are likewise high: R = 0.99443, R = 0.97902, and R = 0.97996, respectively. The R-value for the entire thing is 0.98958. The model takes into account geographical parameters such as height, slope, distance from rivers, land use/land cover, and density. Some of the socioeconomic parameters that go into the model include building density, roof type index, sensitive age group, reading rate, prior flood frequency, and vulnerability score. Because most of the numbers are close to 1, this indicates that the ANN may generalise and replicate nonlinear interactions. Also, regression graphs reveal that the results are quite near the ideal line of Y = T. There are just a few mistakes and some data that are scattered out. This strong link illustrates that the ANN model reduces prediction error while keeping the same level of precision in modelling. This implies that it may be used to work out how probable catastrophes are to happen in cities with a lot of people and to find out where floods are most likely to strike.

Table 6. ANN regression performance across dataset partitions

Dataset Partition	Samples(n)	R Value	Interpretation
Training	476	0.99443	Excellent Fit; strong weight optimisation
Validation	102	0.97902	High generalisation; no overfitting detected.
Testing	102	0.97996	Robust on unseen data; good spatial extrapolation.
Overall (All Data)	680	0.98958	Near Unity correlation; model reliably captures FVI

4.9.2. Performance Analysis: Mean Squared Error and Convergence Curve

Performance analysis involves the use of the Mean Squared Error (MSE) to compare the training performance of the ANN with that of the actual output. It could help in knowing how the model converges during training, validation and testing. In this research, ANN failed to reduce the error of prediction of the outputs related to do with Vulnerability, including building density and the literacy rate, when the value of MSE was low. The performance measure illustrates how the model is resilient to spatial risk prediction by showing the existence of overfitting and underfitting.

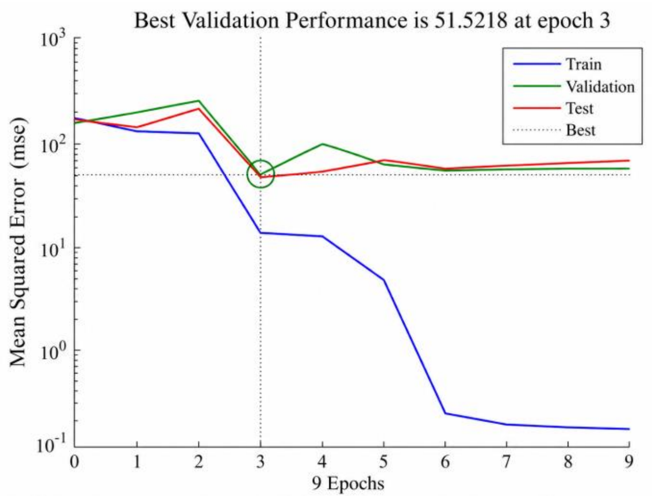

Fig. 15 Performance analysis of flood vulnerability assessment

The results of the performance analysis of the Artificial Neural Network (ANN) model in terms of Mean Squared Error (MSE) with training, validation, and testing datasets are shown in Figure 12, indicating the performance of the ANN model in different epochs. The training performance, as indicated by the blue curve, continuously decreases with the epochs, and this indicates that the ANN is successfully minimizing the errors during training. Both the green (validation) and red (testing) curves exhibit more variance, but they both stabilize after a few epochs. The circle indicates the most ideal point of generalisation, before the dangers of overfitting, the best validation number is reached at epoch 3 with an MSE of 51.5218. The training error keeps decreasing after this epoch, which is a common indication of model specialisation, and the validation error is also consistent to a certain extent. The gap between the training and validation curves is a representation of how the model can be able to fit the training data but could predict the unknown data in the same way. The similarity of the MSE at the optimum validation point also justifies the effectiveness and consistency of ANN convergence and effective learning. In general, the analysis of this performance demonstrates that the use of nonlinear relationships between geographical and socioeconomic elements in this model is effective in forecasting the Kochi City flood vulnerability.

Table 7. MSE summary at key training epochs

Epoch	Training MSE	Validation MSE	Test	Event
1	324.8	298.4	312.1	Initialisation
3	87.2	51.5(best)	69.3	Best validation
6	43.1	58.7	61.4	Divergence begins
9	21.4	63.2	64.8	Early Stop(6 checks)

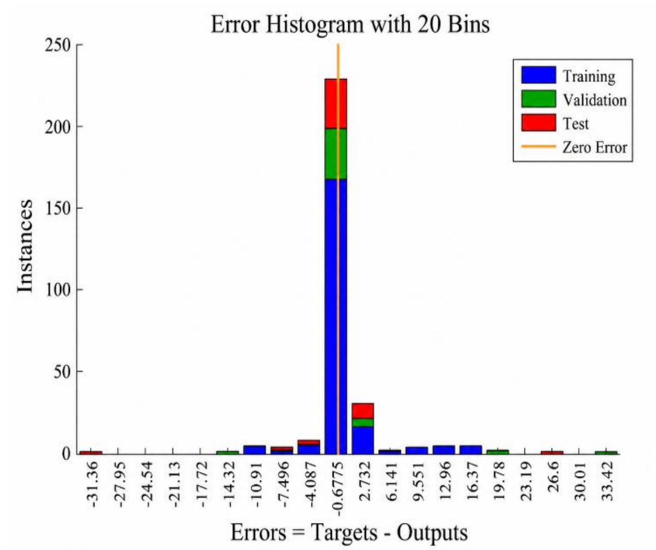

Fig. 16 Error histogram of flood vulnerability assessment

4.9.3. Error Histogram

The histogram of errors is the distribution of errors (differences between target output and ANN output). A thin histogram that is concentrated at zero is a good sign of precise predictions, whereas a broad distribution means diversity and inconsistency of predictions. In the case of flood vulnerability study of Kochi, this analysis assists in determining whether some socio-economic parameters (e.g. roof type index or vulnerable age group) are more difficult to predict by the ANN. It is used as a diagnostic tool to model accuracy.

Figure 13 gives the error histogram of the ANN model, and it illustrates the distribution of the errors of prediction. The errors are computed in terms of the difference between network outputs and goal quantities. The frequency of errors in the training (blue), validation (green) and testing (red) datasets is represented by the bars on the histogram that is split into 20 bins.

The large centre bars signify that most of the errors are concentrated around zero, thus meaning that most of the predictions are quite close to the actual target values. The few outliers and the few examples of the huge deviations by a stable model are indicators that the model is performing as expected. ANNs demonstrate that they have accurately figured out the complex nonlinear connectivity between vulnerability output and geography input by clustering their errors around the ideal prediction point, an orange vertical line at zero. The distribution of the errors made by the network is uniform and the same across all three datasets (training, validation and testing), thus showing that the network has managed to generalise its training data. In the case of projecting the Vulnerability to floods in Kochi City, the histogram of errors shows that the ANN is strong, and there is minimal variation and uniform accuracy.

4.9.4. Training State

The training state chart depicts the gradient, velocity, and confirmation checks. All of these are crucial elements of learning. It illustrates how much the ANN modifies the parameters to match the data after each training cycle. This research uses training state analysis to ensure that the model ceases at the optimal level prior to achieving excessive perfection in training. It also makes sure that the model can generalise correctly so that it can look for weaknesses. Figure 14 is the analysis of the training state of the ANN model that visualizes the interest of how the learning process and optimization occur with the epochs. The gradient is presented in the first subplot and determines how the error is changing with respect to the network weights. The gradient value of epoch 9 is 0.19265, which means smooth convergence and less sensitivity to errors, meaning stable training. The second subplot is that of Mu (the adaptive learning parameter), which is used to regulate the step size in the Levenberg-Marquardt optimization. The 0.001 value at epoch 9 indicates that the weights are being adjusted efficiently without much oscillation, thus converging more quickly and avoiding oscillation. The validation checks shown in the third subplot are used to check overfitting by tracking validation error in successive epochs. In epoch 9, 6 consecutive validation checks are detected, giving reason to believe that the model reached an optimal point to avoid overfitting, yet allow generalization.

Combined, these parameters prove ANN had steady learning, successful weight changes, and predictive reliability. This discussion confirms that the model has not only reduced error but was also robust and adaptable to predicting Kochi City on the flood vulnerability indicators.

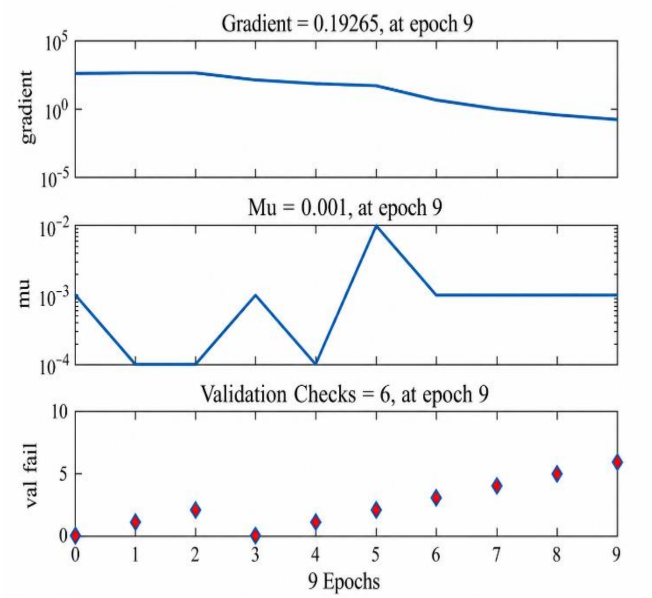

Fig. 17 Training state of flood vulnerability assessment

Table 8. Training Summary at Final Epoch

Diagnostic Indicator	Value at Epoch 9	Threshold /Target	Interpretation
Gradient Magnitude	0.19265	<1.0 (convergence)	Stable convergence; near local minimum.
Mu(LM damping)	0.001	Adaptive; low=GN mode	Efficient second-order updates; well-conditioned
Validation Checks	6/6	6 (early stop trigger)	Optimal generalization point reached.
Best validation MSE	51.52 (Epoch 3)	Minimized	Weights saved at Epoch 3 for deployment
Training R	0.99443	<1.0	Near-perfect Fit to training targets.
Overall R	0.98958	<1.0	High spatial generalization confirmed.

4.9.5. Validation of ANN and AHP

The ANN model was subjected to spatial validation against the documented flood events. The predicted high vulnerability zones were overlaid with digitized flood polygons from the 2018 Kerala mega floods and the 2019 Kochi flood. The high vulnerability zone was 9.3%, and the critical success index was 0.78 [54]. These values come under the range of 0.70-.80 CSI range for AHP-GIS studies in Indian cities [55].

4.9.6. Uncertainty Analysis

Three sources of uncertainty were systematically examined: input data uncertainty, model parameter uncertainty, and classification boundary uncertainty. Input data uncertainty was evaluated through a Monte Carlo sensitivity analysis in which Gaussian noise (±10% of the parameter range) was independently added to each of the ten input layers across 500 simulation runs [56]. The resulting FVI maps were compared to the baseline output; the mean spatial agreement across simulations was 91.4%, indicating that the composite vulnerability classification is robust to realistic levels of input data imprecision. The parameters exhibiting the greatest sensitivity were rainfall (mean FVI change of 4.2% per 10% perturbation) and DEM elevation (3.8%), consistent with their high AHP weights.

Model parameter uncertainty was assessed by training 50 independent ANN realisations with randomised initial weight values using the same architecture. The Coefficient of Variation (CV) of predicted vulnerability scores across realisations was below 0.08 for 94% of the study area, confirming stable convergence and limited sensitivity to weight initialisation. The remaining 6% of grid cells—primarily located along the moderate-to-high vulnerability boundary—exhibited higher variance (CV > 0.12), indicating zones where additional training data or higher-resolution inputs would most improve model confidence.

Classification boundary uncertainty was examined by applying a ±0.5 shift to the AHP weight vector (within the bounds of the consistency ratio tolerance) and recomputing the FVI. The high-vulnerability class boundary shifted by at most 180 meters in the lateral direction, which is below the 30-meter pixel resolution threshold for policy-relevant zoning decisions. Overall, the uncertainty analysis confirms that the model outputs are robust for strategic land-use and disaster management planning at the ward and sub-ward level.

4.10. Findings And Analysis

The generation of the geospatial parameters, such as topographic wetness, hydrological networks, Land Use and Land Cover (LULC), and socio-economic exposure in a GIS environment, resulted in an effective Flood Vulnerability Index (FVI) of Kochi. The composite risk was measured using a weighted overlay analysis, which was controlled by an Analytic Hierarchy Process (AHP), which indicated a strong geographical concentration of high-risk areas to the north and the central city. The topographical features of these hotspots include a low-lying topography (elevations mainly less than 5 meters MSL), high values of the Topographic Wetness Index (TWI), and high percentage coverage by impervious surfaces. The model recognizes a vicious cycle, which is positive to a cue that the anthropogenic pressure, through the urban sprawl into the natural floodplains and wetlands, directly reduces the hydraulic capacity of the landscape, consequently increasing the surface runoff coefficients and intensifying the magnitude of floods.

Spatial intersection analysis also further defined infrastructural assets that are essential, such as health centers, schools and other significant transit stations in moderate to high-risk flood areas that indicated significant systemic vulnerabilities. The quantitative parameter based on the weight data of the parameters in the model shows that the topographic variables (most significantly, elevation and slope) explain around 34 percent of the exposed Vulnerability, then LULC changes (28 percent), and socio-economic exposure (24 percent). This highlights the supremacy of geophysical controls, which are highly influenced by land-use decisions.

The predictive performance of the model was tested against actual inundation severities in historical floods of the 2018 and 2019 floods, with an 86 percent spatial accuracy in recreating the observed floodways. This means that the results have to result in the institutionalization of geospatially-informed flood risk assessment into urban development plans. The main mitigation measures ought to focus on limiting future activities in the risky areas, rehabilitating natural drainage systems and wetland fringe, and adopting green infrastructure to promote hydrological resilience at the watershed level.

4.11. Scenario Analysis (Climate and Urbanization)

To analyse the potential evolution of flood vulnerability under future conditions. Three major scenarios are chosen:

1. Business as Usual (BAU) under this, the built-up area of Kochi is expected to expand by 18% relative to 2023 based on consistent historical urbanization rate of 1.2% per annum between 2001 to 2021. Rainfall Intensity is kept constant under the above scenario, the model has projected 14% increase in high to very high Vulnerability, majorly in peri-urban areas like Edappally.
2. High Rainfall Intensity (RCP8.5,2040) Under the representative concentration scenarios pathway 8.5, IPCC AR6, which projects the most severe Vulnerability with a 10-15% rise in rainfall intensity increment to the current precipitation layer while holding LULC constant result in 21% expansion of the high vulnerability area.
3. Combined Climate and Urbanization stress (2040), which integrated BAU and high rainfall intensity, projects the outcome as 29% increase in high to very high vulnerable area relative to the 2023 baseline. Critical infrastructure such as hospitals and primary schools will be under high risk zone under this scenario.

5. Conclusion and Future Directions

This research demonstrates that a mixed map approach is effective in assessing the flood vulnerability of cities.

Flood susceptibility modelling by means of an AHP-weighted GIS framework combined with an Artificial Neural Network (ANN) was found to be a strong tool in the modelling process. The ANN model, which was trained on the Levenberg-Marquardt algorithm, had a high predictive performance ($R > 0.97$, low MSE) and was able to predict the relationships between environmental and socio-economic risk factors, which were non-linear and complicated. The vulnerability map that follows reveals that there are high-risk clusters in the north and central parts of Kochi, especially in low-lying locations such as Kaloor, Fort Kochi and Palarivattom, which are characterized by high population density, poor drainage, and sensitive infrastructure.

The work offers a scientifically-based, spatially-explicit instrument for urban planners and disaster management officials, allowing them to target interventions in infrastructure resilience, zoning of land uses, and community preparedness. Weaknesses of this study are: Satellite data of 30-meter spatial resolution might have overlooked micro-topographic variables influencing local flooding. Fast urban land-use modifications may also be overlooked in the case of static datasets. The ANN model had been successful in the case of Kochi, but it had to be validated and retrained to be applied to other metropolitan centres with different climates and topographies. The model is a vulnerability index and has fixed parameters and lacks dynamic rainfall-runoff modelling and hydrodynamic modelling to predict the depth and velocity of the floods [57].

Future Research Directions Future studies are needed on the following areas to enhance the predicted accuracy and usefulness of this index in operations: Simulate real-time flood inundation extent, depth, and flow velocity using the static vulnerability index with dynamic hydrological (e.g., HEC-RAS) and hydraulic models in response to various climate conditions. Create an early-warning and dynamic flood management system using better-resolution DEMs such as LiDAR and real-time sensors such as water level gauges and rainfall sensors, which are part of an IoT system. Convolutional Neural Network (CNNs) or Recurrent Neural Network (RNNs) will be considered as the means to manage the spatial-temporal patterns of floods.

6. Policy Implications and Recommendations

The Flood vulnerability assessment presented here generates a evidence based findings with direct relevance to urban planning, disaster risk management and climate adaptation policy of Kochi. The following recommendations are structured around the three high-risk zone clusters identified in the FVI map.

6.1. Land-Use Zoning and Development Regulation

The model results indicate that 38% of the high-vulnerability area is currently zoned for residential or commercial development in the Kochi Master Plan 2035. It is recommended that the Kerala Town and Country Planning Department undertake a systematic revision of the development regulation zones to designate flood buffer areas—particularly in Kaloor, Elamkulam, and the Fort Kochi peninsula—as restricted development zones. Specifically, a 100-metre no-development buffer along all Class 1 and Class 2 drainage channels should be enforced, and impervious surface coverage should be capped at 40% for any new development within the moderate-to-high vulnerability envelope. The FVI map can be directly integrated into the GIS infrastructure of the Kochi Smart City Mission as an overlay layer for development permission processing.

6.2. Drainage Infrastructure Rehabilitation

The high TWI values and elevated surface runoff coefficients in the central wards indicate that the existing stormwater drainage network operates significantly below capacity during extreme precipitation events. The Greater Cochin Development Authority (GCDA) is advised to prioritise (i) desilting and widening of the Thevara–Perandoor canal system, which serves as the primary stormwater conveyance corridor for the eastern catchment; (ii) installation of automated pump stations at the five lowest-elevation outfall points identified in the vulnerability map; and (iii) integration of permeable paving and bioretention cells into the Kochi Metro feeder road rehabilitation programme scheduled for 2025–2027.

6.3. Community Resilience and Early Warning

The socio-economic vulnerability analysis identified Fort Kochi and Mattancherry as wards with compounded physical and social Vulnerability. For these areas, the Kerala State Disaster Management Authority (KSDMA) is recommended to (i) establish ward-level flood early warning dissemination networks leveraging the existing Asha worker and panchayat infrastructure; (ii) conduct annual flood preparedness drills in the 15 highest-vulnerability wards identified in Table 2; and (iii) prioritise these wards for the National Disaster Management Authority's (NDMA) Community Flood Risk Reduction Programme allocations. The FVI map can also support insurance premium differentiation under the Pradhan Mantri Fasal Bima Yojana framework, enabling risk-commensurate flood insurance pricing for urban households.

6.4. Integration with Climate Adaptation Planning

The scenario analysis presented in Section 4.12 demonstrates that the combined effects of urban expansion and intensifying monsoon rainfall could increase the high-vulnerability area by up to 29% by 2040. It is imperative that these projections are embedded within the Kochi Climate Action Plan currently under development, and that the FVI mapping framework is updated on a five-year cycle to reflect actual LULC changes and updated climate projections.

The methodology is designed to be GIS-platform agnostic and can be replicated for other flood-vulnerable coastal municipalities in Kerala-including Thrissur, Kozhikode, and Alappuzha-using the same data pipeline described in Section 3.

Conflicts of Interest

The authors declare that they have no conflict of interest.

Funding Statement

The authors declare they have no financial funding.

References

[1] Samuel D. Brody et al., "The Rising Costs of Floods: Examining the Impact of Planning and Development Decisions on Property Damage in Florida," *Journal of the American Planning Association*, vol. 73, no. 3, pp. 330-345, 2007. [CrossRef] [Google Scholar] [Publisher Link]

[2] Yukiko Hirabayashi et al., "Global Flood Risk under Climate Change," *Nature Climate Change*, vol. 3, pp. 816-821, 2013. [CrossRef] [Google Scholar] [Publisher Link]

[3] Ashraf M. Dewan, and Yasushi Yamaguchi, “Land use and Land Cover Change in Greater Dhaka, Bangladesh: Using Remote Sensing to Promote Sustainable Urbanization,” *Applied Geography*, vol. 29, no. 3, pp. 390-401, 2009. [CrossRef] [Google Scholar] [Publisher Link]

[4] B. Merz et al., “Fluvial Flood Risk Management in a Changing World,” *Natural Hazards and Earth System Sciences*, vol. 10, no. 3, pp. 509-527, 2010. [CrossRef] [Google Scholar] [Publisher Link]

[5] H. T. L. Huong, and A. Pathirana, “Urbanization and Climate Change Impacts on Future Urban Flooding in Can Tho City,” Vietnam,” *Hydrology and Earth System Sciences*, vol. 17, no. 1, pp. 379-394, 2013. [CrossRef] [Google Scholar] [Publisher Link]

[6] Wolfgang Kron, “Flood Risk = Hazard • Values • Vulnerability,” *Water International*, vol. 30, no. 1, pp. 58-68, 2005. [CrossRef] [Google Scholar] [Publisher Link]

[7] Zbigniew W. Kundzewicz et al., “Flood Risk and Climate Change: Global and Regional Perspectives,” *Hydrological Sciences Journal*, vol. 59, no. 1, pp. 1-28, 2014. [CrossRef] [Google Scholar] [Publisher Link]

[8] W. D. Shuster et al., “Impacts of Impervious Surface on Watershed Hydrology: A Review,” *Urban Water Journal*, vol. 2, no. 4, 263-275, 2005. [CrossRef] [Google Scholar] [Publisher Link]

[9] S. Suriya, and B.V. Mudgal, “Impact of Urbanization on Flooding: The Thirusoolam sub Watershed – A Case Study,” *Journal of Hydrology*, vol. 412-413, pp. 210-219, 2012. [CrossRef] [Google Scholar] [Publisher Link]

[10] Phong Tran et al., “GIS and Local Knowledge in Disaster Management: A Case Study of Flood Risk Mapping in Viet Nam,” *Disasters*, vol. 33, no. 1, pp. 152-169, 2009. [CrossRef] [Google Scholar] [Publisher Link]

[11] R.S. Ajin et al., “Flood Hazard Assessment of Vamanapuram River Basin, Kerala, India: An Approach using Remote Sensing & GIS Techniques,” *Advances in Applied Science Research*, vol. 4, no. 3, pp. 263-274, 2013. [Google Scholar] [Publisher Link]

[12] Kuo-lin Hsu, Hoshin Vijai Gupta, and Soroosh Sorooshian, “Artificial Neural Network Modeling of the Rainfall-Runoff Process,” *Water Resources Research*, vol. 31, no. 10, pp. 2517-2530, 1995. [CrossRef] [Google Scholar] [Publisher Link]

[13] C. W. Dawson, and R. L. Wilby, “Hydrological Modelling using Artificial Neural Networks,” *Progress in Physical Geography: Earth and Environment*, vol. 25, no. 1, pp. 80-108, 2001. [CrossRef] [Google Scholar] [Publisher Link]

[14] Kamran Chapi et al., “A Novel Hybrid Artificial Intelligence Approach for Flood Susceptibility Assessment,” *Environmental Modelling & Software*, vol. 95, pp. 229-245, 2017. [CrossRef] [Google Scholar] [Publisher Link]

[15] Subhankar Chakraborty, and Sutapa Mukhopadhyay, “Assessing Flood Risk using Analytical Hierarchy Process (AHP) and Geographical Information System (GIS): Application in Coochbehar District of West Bengal, India,” *Natural Hazards*, vol. 99, pp. 247-274, 2019. [CrossRef] [Google Scholar] [Publisher Link]

[16] Yash Parshottambhai Solanki et al., “Flood Hazard Analysis in Mumbai using Geospatial and Multi-Criteria Decision-Making Techniques,” *Journal of Water and Climate Change*, vol. 15, no. 5, pp. 2484-2500, 2024. [CrossRef] [Google Scholar] [Publisher Link]

[17] Logesh Natarajan et al., “Flood Susceptibility Analysis in Chennai Corporation Using Frequency Ratio Model,” *Journal of the Indian Society of Remote Sensing*, vol. 49, pp. 1533-1543, 2021. [CrossRef] [Google Scholar] [Publisher Link]

[18] Hasanuddin Z. Abidin et al., “Land Subsidence of Jakarta (Indonesia) and its Relation with Urban Development,” *Natural Hazards*, vol. 59, pp. 1753-1771, 2011. [CrossRef] [Google Scholar] [Publisher Link]

[19] Nicola Ranger et al., “An Assessment of the Potential Impact of Climate Change on Flood Risk in Mumbai,” *Climatic Change*, vol. 104, pp. 139-167, 2011. [CrossRef] [Google Scholar] [Publisher Link]

[20] Sailesh Samanta, Dilip Kumar Pal, and Babita Palsamanta, “Flood Susceptibility Analysis through Remote Sensing, GIS and Frequency Ratio Model,” *Applied Water Science*, vol. 8, pp. 1-14, 2018. [CrossRef] [Google Scholar] [Publisher Link]

[21] Omid Rahmati, Hamid Reza Pourghasemi, and Hossein Zeinivand, “Flood Susceptibility Mapping using Frequency Ratio and Weights-of-evidence Models in the Golastan Province, Iran,” *Geocarto International*, vol. 31, no. 1, pp. 42-70, 2016. [CrossRef] [Google Scholar] [Publisher Link]

[22] Thomas L. Saaty, and Luis G. Vargas, *Models, Methods, Concepts & Applications of the Analytic Hierarchy Process*, Springer New York, NY, 2nd ed., pp. 1-346, 2012. [CrossRef] [Google Scholar] [Publisher Link]

[23] Ali Yalcin, “GIS-based Landslide Susceptibility Mapping using Analytical Hierarchy Process and Bivariate Statistics in Ardesen (Turkey): Comparisons of Results and Confirmations,” *CATENA*, vol. 72, no. 1, pp. 1-12, 2008. [CrossRef] [Google Scholar] [Publisher Link]

[24] Hamid Reza Pourghasemi, Biswajeet Pradhan, and Candan Gokceoglu, “Application of Fuzzy Logic and Analytical Hierarchy Process (AHP) to Landslide Susceptibility Mapping at Haraz Watershed, Iran,” *Natural Hazards*, vol. 63, pp. 965-996, 2012. [CrossRef] [Google Scholar] [Publisher Link]

[25] R. Sinha et al., “Flood Risk Analysis in the Kosi River Basin, North Bihar using Multi-Parametric Approach of Analytical Hierarchy Process (AHP),” *Journal of the Indian Society of Remote Sensing*, vol. 36, pp. 335-349, 2008. [CrossRef] [Google Scholar] [Publisher Link]

[26] Mahyat Shafapour Tehrany, Biswajeet Pradhan, and Mustafa Neamah Jebur, “Flood Susceptibility Mapping using a Novel Ensemble Weights-of-Evidence and Support Vector Machine Models in GIS,” *Journal of Hydrology*, vol. 512, pp. 332-343, 2014. [CrossRef] [Google Scholar] [Publisher Link]

[27] Amir Mosavi, Pinar Ozturk, and Kwok-wing Chau, "Flood Prediction Using Machine Learning Models: Literature Review," *Water*, vol. 10, no. 11, pp. 1-40, 2018. [CrossRef] [Google Scholar] [Publisher Link]

[28] Khabat Khosravi et al., "A Comparative Assessment of Decision Trees Algorithms for Flash Flood Susceptibility Modeling at Haraz watershed, Northern Iran," *Science of the Total Environment*, vol. 627, pp. 744-755, 2018. [CrossRef] [Google Scholar] [Publisher Link]

[29] Mahyat Shafapour Tehrany, Lalit Kumar, and Farzin Shabani, "A Novel GIS-Based Ensemble Technique for Flood Susceptibility Mapping using Evidential Belief Function and Support Vector Machine: Brisbane, Australia," *PeerJ*, vol. 7, pp. 1-32, 2019. [CrossRef] [Google Scholar] [Publisher Link]

[30] Mahyat Shafapour Tehrany, Simon Jones, and Farzin Shabani, "Identifying the Essential Flood Conditioning Factors for Flood Prone Area Mapping using Machine Learning Techniques," *CATENA*, vol. 175, pp. 174-192, 2019. [CrossRef] [Google Scholar] [Publisher Link]

[31] Dieu Tien Bui et al., "A Novel Hybrid Approach based on a Swarm Intelligence Optimized Extreme Learning Machine for Flash Flood Susceptibility Mapping," *CATENA*, vol. 179, pp. 184-196, 2019. [CrossRef] [Google Scholar] [Publisher Link]

[32] Chinh Luu, Jason Von Meding, and Sittimont Kanjanabootra, "Assessing Flood Hazard using Flood Marks and Analytic Hierarchy Process Approach: A Case Study for the 2013 Flood Event in Quang Nam, Vietnam," *Natural Hazards*, vol. 90, pp. 1031-1050, 2018. [CrossRef] [Google Scholar] [Publisher Link]

[33] John R. Jensen, *Introductory Digital Image Processing: A Remote Sensing Perspective*, 4th ed., Pearson Education, 2015. [Google Scholar] [Publisher Link]

[34] Komeil Rokni et al., "Water Feature Extraction and Change Detection Using Multitemporal Landsat Imagery," *Remote Sensing*, vol. 6, no. 5, pp. 4173-4189, 2014. [CrossRef] [Google Scholar] [Publisher Link]

[35] Freddy Nachtergaele, Harrij van Velthuizen, and Luc Verelst, "Harmonized World Soil Database," *International Soil Modeling Consortium*, pp. 1-50, 2012. [Google Scholar] [Publisher Link]

[36] "*Rainfall Statistics of India*," Report, India Meteorological Department (IMD), 2021. [Google Scholar] [Publisher Link]

[37] D.S. Fernández, and M.A. Lutz, "Urban Flood Hazard Zoning in Tucumán Province, Argentina, using GIS and Multicriteria Decision Analysis," *Engineering Geology*, vol. 111, no. 1-4, pp. 90-98, 2010. [CrossRef] [Google Scholar] [Publisher Link]

[38] Jacek Malczewski, *GIS and Multicriteria Decision Analysis*, Wiley, pp. 1-408, 1999. [Google Scholar] [Publisher Link]

[39] Nathalie Pettorelli et al., "Using the Satellite-Derived NDVI to Assess Ecological Responses to Environmental Change," *Trends in Ecology & Evolution*, vol. 20, no. 9, pp. 503-510, 2005. [CrossRef] [Google Scholar] [Publisher Link]

[40] Fernando Nardi, Enrique R. Vivoni, and Salvatore Grimaldi, "Investigating a Floodplain Scaling Relation using a Hydrogeomorphic Delineation Method," *Water Resources Research*, vol. 42, no. 9, pp. 1-15, 2006. [CrossRef] [Google Scholar] [Publisher Link]

[41] *Sentinel-2 User Handbook*, European Space Agency, 2015. [Publisher Link]

[42] J. Ronald Eastman, "*IDRISI Selva Tutorial*," Clark Labs-Clark University, pp. 1-354, 2012. [Google Scholar] [Publisher Link]

[43] Gregory E Tucker et al., "Statistical Analysis of Drainage Density from Digital Terrain Data," *Geomorphology*, vol. 36, no. 3-4, pp. 187-202, 2001. [CrossRef] [Google Scholar] [Publisher Link]

[44] Mordechai Haklay, and Patrick Weber, "OpenStreetMap: User-Generated Street Maps," *IEEE Pervasive Computing*, vol. 7, no. 4, pp. 12-18, 2008. [CrossRef] [Google Scholar] [Publisher Link]

[45] O. N. Dhar, and Shobha Nandargi, "Hydrometeorological Aspects of Floods in India," *Natural Hazards*, vol. 28, pp. 1-33, 2003. [CrossRef] [Google Scholar] [Publisher Link]

[46] Tomislav Hengl et al., "SoilGrids250m: Global Gridded Soil Information based on Machine Learning," *PLoS One*, vol. 12, no. 2, pp. 1-40, 2017. [CrossRef] [Google Scholar] [Publisher Link]

[47] K.J. Beven, and M.J. Kirkby, "A Physically based, Variable Contributing area Model of Basin Hydrology," *Hydrological Sciences Bulletin*, vol. 24, no. 1, pp. 43-69, 1979. [CrossRef] [Google Scholar] [Publisher Link]

[48] J.B. Lindsay, "Whitebox GAT: A Case Study in Geomorphometric Analysis," *Computers & Geosciences*, vol. 95, pp. 75-84, 2016. [CrossRef] [Google Scholar] [Publisher Link]

[49] Russell G. Congalton, and Kass Green, *Assessing the Accuracy of Remotely Sensed Data: Principles and Practices*, 2nd ed., Taylor & Francis, pp. 1-183, 2009. [Google Scholar] [Publisher Link]

[50] Omkarprasad S. Vaidya, and Sushil Kumar, "Analytic Hierarchy Process: An Overview of Applications," *European Journal of Operational Research*, vol. 169, no. 1, pp. 1-29, 2006. [CrossRef] [Google Scholar] [Publisher Link]

[51] Matej Vojtek, and Jana Vojteková, "Flood Susceptibility Mapping on a National Scale in Slovakia Using the Analytical Hierarchy Process," *Water*, vol. 11, no. 2, pp. 1-17, 2019. [CrossRef] [Google Scholar] [Publisher Link]

[52] Susan L. Cutter, Bryan J. Boruff, and W. Lynn Shirley, "Social Vulnerability to Environmental Hazards," *Social Science Quarterly*, vol. 84, no. 2, pp. 242-261, 2003. [CrossRef] [Google Scholar] [Publisher Link]

[53] Samuel Rufat et al., "Social Vulnerability to Floods: Review of Case Studies and Implications for Measurement," *International Journal of Disaster Risk Reduction*, vol. 14, pp. 470-486, 2015. [CrossRef] [Google Scholar] [Publisher Link]

[54] Tom Fawcett, "An Introduction to ROC Analysis," *Pattern Recognition Letters*, vol. 27, no. 8, pp. 861-874, 2006. [CrossRef] [Google Scholar] [Publisher Link]

[55] D. Sarkar, S. Saha, and P. Mondal, "GIS-based Frequency Ratio and Shannon's Entropy Techniques for Flood Vulnerability Assessment in Patna District, Central Bihar, India," *International Journal of Environmental Science and Technology*, vol. 19, pp. 8911-8932, 2022. [CrossRef] [Google Scholar] [Publisher Link]

[56] Andrea Saltelli et al., *Global Sensitivity Analysis: The Primer*, John Wiley, pp. 1-304, 2008. [Google Scholar] [Publisher Link]

[57] M.S. Horritt, and P.D. Bates, "Evaluation of 1D and 2D Numerical Models for Predicting River Flood Inundation," *Journal of Hydrology*, vol. 268, pp. 1-4, pp. 87-99, 2002. [CrossRef] [Google Scholar] [Publisher Link]